JOURNAL OF GEOPHYSICAL RESEARCH, VOL. 88, NO. A11, PAGES 8667-8678, NOVEMBER 1, 1983

SATURN'S UPPER ATMOSPHERE FROM THE VOYAGER 2 EUV SOLAR AND STELLAR OCCULTATIONS

Gerald R. Smith, D.E. Shemansky, J.B. Holberg, A.L. Broadfoot, and B.R. Sandel

Center for Space Sciences, University of Southern California, Tucson Laboratories

John C. McConnell

Department of Physics, York University

Abstract. The temperature and composition of the upper atmosphere of Saturn have been inferred from Voyager 2 ultraviolet spectrometer occultation measurements made by observing the sun and the star δ-Scorpii while they were being occulted by Saturn. The observations analyzed here provide atmospheric parameters from 2900 km down to 960 km above the 1-bar level referred to the equator. The temperature in the model simulation of the data is 420 ± 30 K down to about 1600 km. Below 1600 km the temperature decreases with a variable lapse rate down to 120 ± 30 K near the methane homopause located at 1010 ± 40 km. A constant temperature at 120 K is applied in the model for the region of the methane homopause down to 960 km where the present analysis terminates. Column amounts of H_2 and H were measured from 2900 km down to about 1100 km, giving densities of $[H_2] \sim 1.0 \times 10^8$ cm^{-3} and $[H] \sim 5.5 \times 10^6$ cm^{-3} near the exobase at 2500 km. Near the methane homopause the H_2 density is $[H_2] = 1.2 \times 10^{12}$ cm^{-3} with a CH_4 number density mixing ratio of 6.0×10^{-5}. The eddy diffusion coefficient in the vicinity of the methane homopause is estimated to be $\sim 5.0 \times 10^6$ cm^2 s^{-1}. The atomic hydrogen density profile suggests a downward H flux of $\sim 1.8 \times 10^9$ cm^{-2} s^{-1} from near the exobase down to a terminal boundary of about 1200 km.

Introduction

The upper atmosphere of Saturn has been considered similar to Jupiter's in thermal structure, composition, and photochemistry. Molecular hydrogen was first discovered on Saturn by Munch and Spinrad [1962]. Methane was identified originally by Wildt in the early 1930s [Wildt, 1932] and later reported by Kuiper [1952]. Ethane was detected on Saturn in 1974 [Gillett and Forrest, 1974]. Moos and Clarke [1979] detected acetylene in 1978 by using the IUE satellite.

The thermal structure of Saturn was not well known until the Voyager encounters. Prior to this the effective temperature was set at 95 ± 5 K [Tokunaga, 1978]. The emission peak at 7.9 μm [Tokunaga, 1978, Strobel, 1978] suggested a temperature in the stratosphere greater than 130 K. The Pioneer 11 data indicate a stratosphere temperature of ≃ 125 K [Kliore et al., 1980; Orton and Ingersoll, 1980]. No measurements of the neutral upper atmosphere were made, however, until the Voyager encounters.

Paper number 3A0905.
0148-0227/83/003A-0905$05.00

The preliminary estimate of 850 ± 100 K for the temperature in the upper atmosphere of Saturn based on the Voyager 1 UVS solar occultation [Broadfoot et al., 1981] appears to be too large, caused primarily by a misinterpretation of the effects of an instrument gain change during the occultation [see Smith et al., 1982] and by severe pointing problems. However, preliminary modeling of the Voyager 2 δ-Scorpii (δ-Sco) stellar occultation showed that the temperature was in the neighborhood of 400 K [Sandel et al., 1982b]. Two analyses of the δ-Sco occultation data have been published, the preliminary work by Sandel et al. [1982b] and the Festou and Atreya [1982] analysis. Festou and Atreya [1982] have inferred a temperature of ~800 K in disagreement with the 400 K result of Sandel et al. [1982b].

In this paper we analyze the Voyager 2 solar entrance and δ-Sco exit occultations. The analysis shows that both data sets are consistent with a temperature of ~420 K in the thermosphere and that the larger temperature derived by Festou and Atreya [1982] is not related to problems with data quality. These observations complement each other since the solar occultation measures H_2 column amounts and the H profile high in the thermosphere down to ~1100 km, whereas the stellar occultation measures the H_2 profile in the middle and lower thermosphere as well as CH_4 near the homopause. Thus the two Voyager 2 UVS occultations define the Saturn atmosphere over the altitude range of 2900 km to 960 km above the 1-bar level and provide the only available direct measure of the neutral atmospheric densities and temperature in the region at and above the CH_4 homopause.

The Occultation Observations

The Voyager 2 ultraviolet spectrometer (UVS) is similar to the Voyager 1 instrument and is described by Broadfoot et al. [1977] [see Smith et al. 1982]. The entire wavelength range from 513 to 1680 Å is simultaneously detected by a 128-element anode array. The instrument is capable of working in two modes: a photon-counting mode for dim sources and an analogue (current integration) mode for bright sources. The instrument is designed with two observing ports having different fields of view; the airglow port and the occultation port. The δ-Sco stellar occultation was observed in the photon-counting mode through the airglow port, while the solar occultation was observed in the analogue mode through the occultation port.

The geometry of both the stellar and solar occultations at the Voyager 2 encounter are shown in Figure 1. The solar occultation described

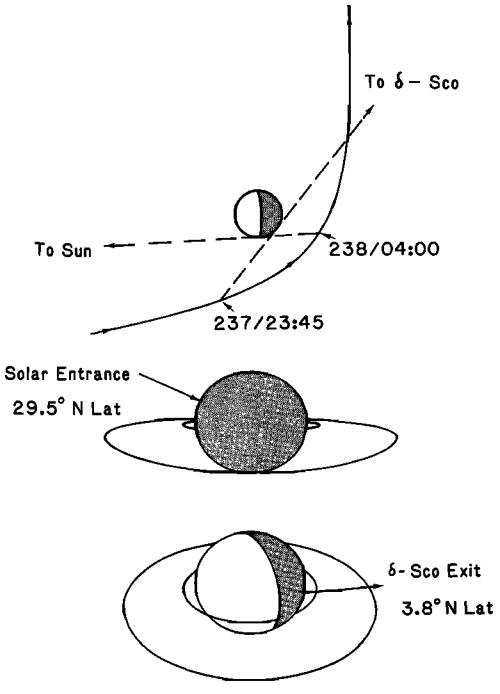

Fig. 1. Geometry of the Voyager 2 occultations at Saturn. The top portion shows the encounter trajectory as viewed from the north pole and spacecraft event times (UT) for the solar and stellar occultations. The middle portion shows the solar entrance occultation as viewed from near the equator and the lower portion is the δ-Sco exit geometry showing the evening terminator.

here occurred between 0400 and 0410 UT on day 238, 1981. During the solar occultation the spacecraft-planet range was 165,000 km, and the spacecraft-sun line crossed Saturn's limb at ~29.5° north latitude. At this range the sun subtends about 150 km in the atmosphere and is imaged on about 2 anodes at a specific wavelength. The radial descent velocity of the spacecraft-sun line through the atmosphere was 19.2 km/s. Since spectra are recorded every 0.32 s, the transmission of the solar flux through the atmosphere was recorded every 6.1 km.

The δ-Sco exit occultation occurred on the dark side of Saturn on day 237, 1981 at 2345 UT. The spacecraft-star line crossed Saturn's limb at 3.8° north latitude with a relative velocity of 10.2 km/s. Since the star is effectively a point source the spatial resolution in Saturn's atmosphere was 3.3 km, which allows a reasonable analysis of the CH_4 homopause region of the atmosphere. The count rate for the unattenuated stellar signal was about 120 counts/s for the peak channels (for spectra see Festou and Atreya [1982]). Since there is no stellar signal below 912 Å, information was not obtained from absorption in the H and H_2 ionization and dissociation continuum. However, information was obtained on H_2 through absorption by the various H_2 discrete bands longward of 912 Å. Since the dominant hydrocarbons also absorb in this wavelength range the stellar occultation provides fairly exact height and temperature information near the homopause.

The basic data returned by the UVS instrument in these observations are count rates per 9.26 Å channel over the wavelength range 513-1680 Å as a function of altitude. Since the instrument is an objective grating spectrometer [Broadfoot et al., 1977] there will be variations due to motion of the spacecraft superimposed on the count rate signal if the source of the signal is not filling the instrument's field of view, especially in the dispersion (0.25° or 0.1°) direction. The occultation port's field is 0.25° x 0.86° and the airglow port is 0.1° x 0.86°, with both ports possessing a triangular slit function in the dispersion direction. The airglow port has a spectral resolution of ~28 Å for point sources and the occultation port with the sun as a source at Saturn has a spectral resolution of ~45 Å. The sun's effective field at Saturn is about 0.05°, and therefore both occultations show signal variation due to spacecraft limit cycle motion. In order to retrieve the transmission signature of the atmosphere the effects of the limit cycle motion must be removed. The attitude control motions of the spacecraft are well known and related in time, provided that the scan platform has not moved relative to the spacecraft. Thus if the location of the source in the field of view is known at a particular time its location at another time can be accurately determined. Spectra recorded when the source is located at different positions in the field of view will be shifted in wavelength, and spectral features show a wavelength shift as well as a count rate difference due to the triangular slit function. Thus if the scan platform has moved, and the source does not fill the field of view, it is possible to locate spectra taken at different times that correspond to the same location of the source in the field of view, by a wavelength correlation of spectral features of the source spectrum, such as the Lyα line for the solar spectrum. With either of the above techniques it is possible to produce a series of 'reference' spectra acquired as the source moves across the field of view during pre or post encounter observations. The raw spectra can then simultaneously be converted from count rate to atmospheric transmission (I/I_∞) and corrected for the position of the source within the field of view by dividing each spectrum in the sequence by the appropriate reference spectrum.

Solar Occultation

Figure 2 shows the raw solar occultation data for the 592 and 1213 Å channels and pointing information obtained from the spacecraft attitude control system. The top panel shows the signal rate, the bottom panel shows the variation of the sun's relative position along the 0.86° length of the slit, and the middle panel shows the sun's relative position along the width (ΔW; the spectrometer's dispersion direction) of the slit (0.25°). The sun was acquired at about 0354 UT and was held until 0400 UT when a scan platform slew was executed. After the slew the UVS field of view drifted, due to spacecraft motion, back across the sun at 0401 UT. We know the sun drifted through the field because the signal went from minimum to maximum and back to minimum,

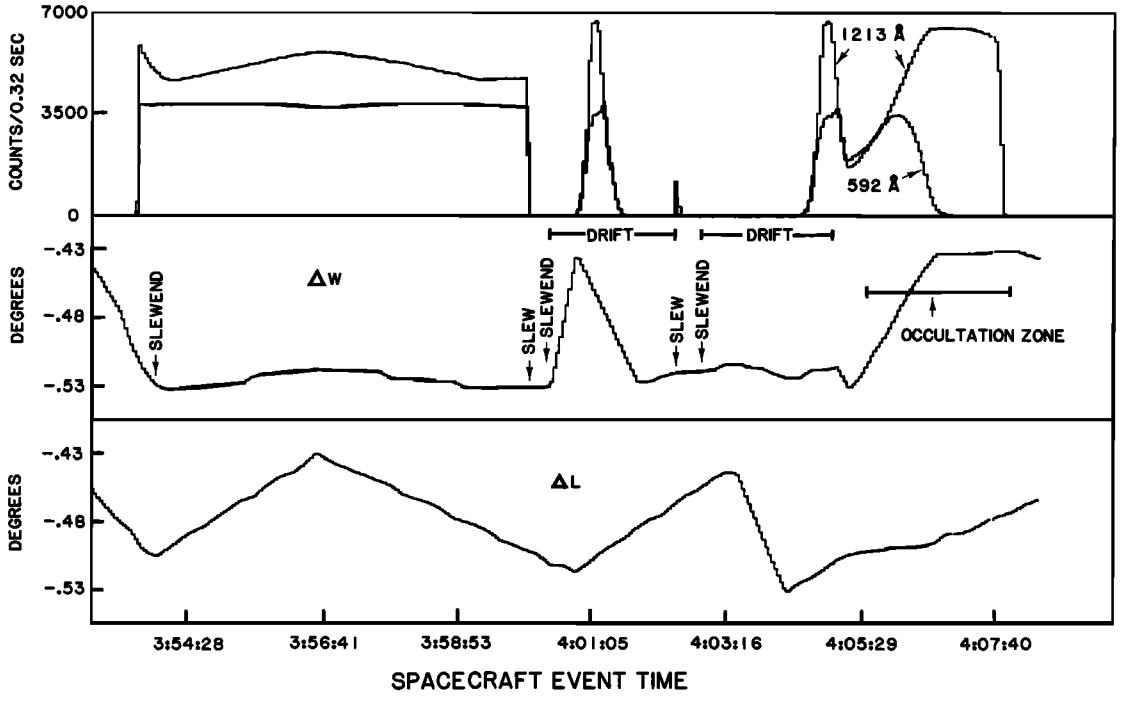

Fig. 2. Unmodified raw data from the solar entrance occultation. The top panel shows the signal counts from two channels from the time of first solar acquisition until complete atmospheric extinction occurred. The middle panel shows the relative motion of the slit in the dispersion direction of the spectrometer (ΔW). We have also shown the various slews and drifts executed by the spacecraft during this time interval. The lower panel shows the relative motion of the slit in the direction of its length (ΔL).

while ΔW was monatonically decreasing (center panel). After another slew and drift the sun was finally acquired at 0405 UT just before atmospheric absorption began. Owing to these various slews separating the drifts marked in Figure 2, the pointing from one drift has no direct relation to the pointing from another area. The middle panel shows that the sun remained near the center of the field of view, since the signal is at a maximum in the 1213 Å channel, from 0406:33 UT until near the end of the occultation. This fact and the reference spectra provided by the drifting of the field of view completely over the sun at 0401 UT allowed a successful data analysis for the entire occultation.

Thus, in order to convert the raw solar data into transmission (I/I_o) information for the count rate spectra we cross-correlated the Lyα channels from the reference (I_o) data acquired at time 0401 UT (see Figure 2), where the sun moved completely through the field of view, spectrum by spectrum with the Lyα channels from the data at times 0405 UT to 0406:33 UT. Thus a sequence of I_o reference spectra were obtained that correspond to the same position of the source in the instrument's field of view. These reference spectra were then divided into the corresponding 'atmospheric' spectra. For times greater than 0406:33 UT we used the same reference spectrum obtained for time 0406:33 UT. This is permissible since the sun's position with respect to ΔW was essentially constant for times greater than 0406:33 U.T. This process essentially removed the variation in the signal caused by the motion of the sun within the field of view, and gives a sequence of I/I_o spectra containing the absorption signature of the atmosphere. The results of the above procedure are quite satisfactory as is shown in Figure 3 where we display transmission curves of representative regions of the spectrum.

Stellar Occultation

At the time of the δ-Sco occultation the spacecraft was relatively deep in Saturn's magnetosphere and the charged particle environment induced a higher than normal dark count rate. This was removed by subtracting a background spectrum obtained when the UVS field of view was completely on the shadowed disc of Saturn prior to the stellar exit. Since the stellar spectra contained no measureable signal shortward of the HI Lyman limit at 912 Å, monitoring the level of the relatively flat dark count spectrum is straightforward. During the atmospheric occultation this background remained constant.

At the time of the stellar occultation the normal spacecraft limit cycle caused the star to exhibit a periodic cyclic motion of approximately 0.1^o amplitude with respect to ΔW with a ~10 min period. The error signals from the spacecraft attitude control system were used to ascertain the position of the star within the UVS field of view with an accuracy of 0.002^o in the dispersion direction (ΔW). The effect of this cyclic motion was removed from the data by establishing an array of unattenuated reference stellar spectra (I_o) obtained 72 days later. This observation

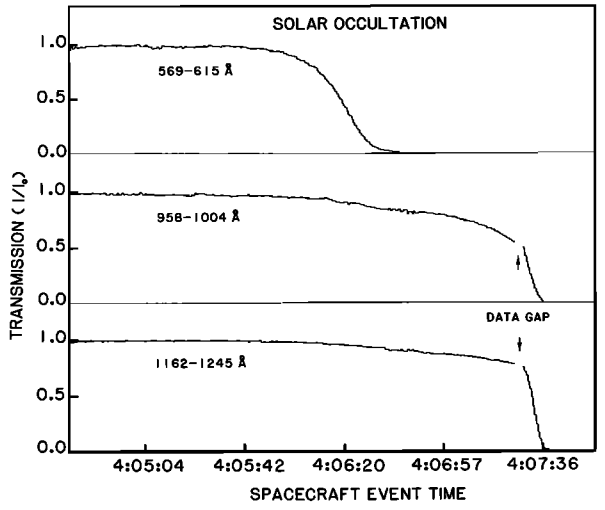

Fig. 3. The data from the solar occultation for three wavelength bands after the various reduction procedures were applied (see text). The data are given as transmission curves as a function of the spacecraft event time given in UT.

consisted of scans that allowed the star to move across the UVS field of view in the dispersion direction at a resolution of 0.002°. The star was observed on axis several times during the subsequent Saturn ring occultation through clear portions of the rings [Holberg et al., 1982a] and these were compared with the stellar I_o spectra. There was found to be no change in the observed spectra from these different times. The Voyager 2 instrument stability appears to be within 4% over a two year span from 1978 to 1980 [see Holberg et al., 1982b], and this procedure is considered to be valid by any reasonable standard. The occultation spectra (I) were then subjected to a channel by channel division of the appropriate reference spectrum obtained while the source was in the same position in the field of view as the occultation spectrum. The sequence of I/I_o spectra thus obtained has the absorption signature of the various atmospheric constituents. Figure 4 shows the transmission curve for the 939-1041 Å band of the stellar occultation. The data just before and just after the data gap show some discontinuity. This area happens to be right at the end of a limit cycle where relative positions are most difficult to ascertain, and the uncertainty in this region of I/I_o is at least 5% and could be as high as 10%. An example of the removal of limit cycle modulation from occultation data can be found in Holberg et al., [1982a], where a technique similar to that used here was employed in the reduction of the 2 hours of δ-Sco ring occultation data obtained immediately after the atmospheric exit discussed here.

Spectral Region Shortward of 912 Å

Below a wavelength of about 850 Å, continuous absorption by molecular hydrogen should be the primary source of atmospheric extinction. The region between 850 Å and 912 Å Lyman limit can be used to obtain information about atomic hydrogen. However, the discrete H_2 bands also absorb in this region so that the molecular hydrogen profile must be determined first before an estimate of H densities can be made.

The attenuated radiation as measured by the UVS can be written as

$$I(\lambda) = I_o(\lambda) \exp(-\tau_s(\lambda)) \qquad (1)$$

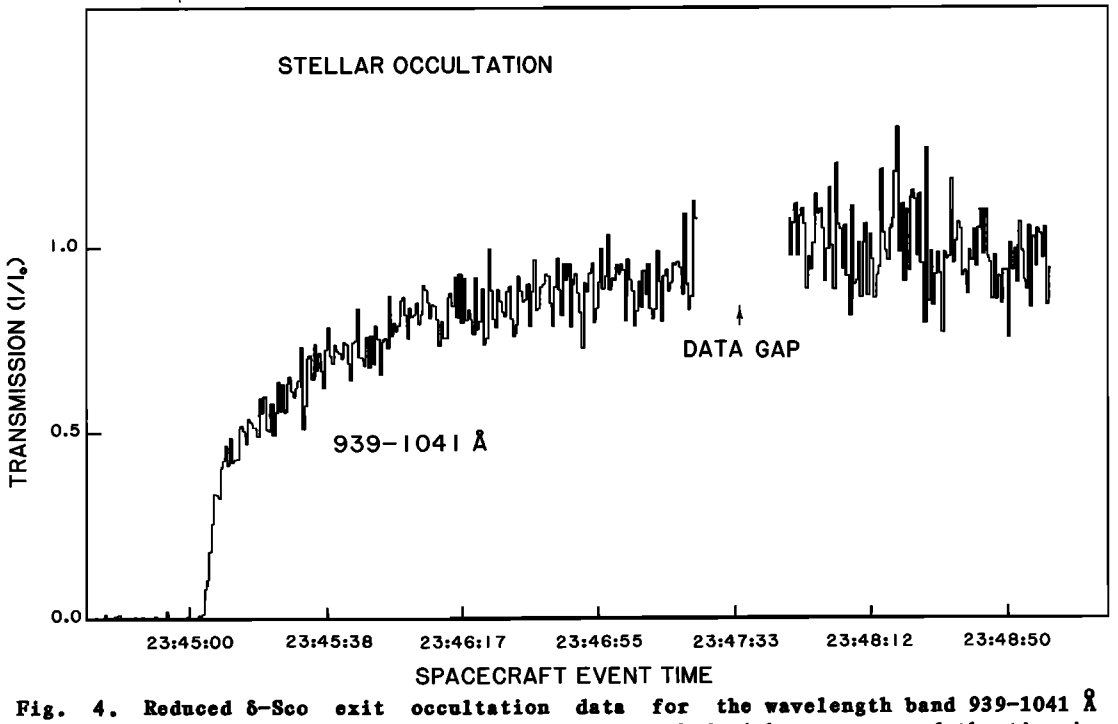

Fig. 4. Reduced δ-Sco exit occultation data for the wavelength band 939-1041 Å given as a transmission curve. A data gap is marked with an arrow and the time is spacecraft event time given in UT.

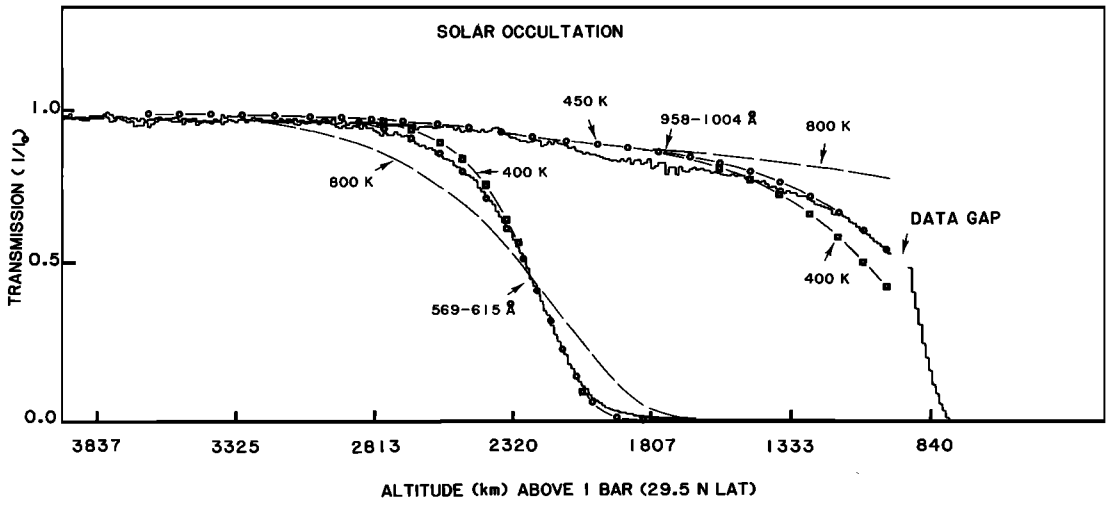

Fig. 5. Comparison of 400 K, 450 K and 800 K models with the Voyager 2 solar occultation data from the wavelength regions 569-615 Å and 958-1004 Å. The data are the solid (histogram) lines and the isothermal models are 450 K (open circles), 400 K (squares), and 800 K (dashed line). The data and models are given as transmission curves as a function of altitude above the 1-bar level at 29.5° N latitude. The data are plotted as a histogram with each point representing the information from two spectra or about 12 km. For the 958-1004 Å data there is little difference in the three models above 1800 km.

where $I_o(\lambda)$ is the unattenuated intensity of the source at wavelength λ. From equation (1) and Chamberlain [1963] we obtain

$$\tau_s(\lambda) = -\ln(I/I_o) \simeq \tau_o(\lambda) \exp\frac{r - r_o}{H} \quad (2)$$

$$\tau_o(\lambda) \simeq n(r_o)\sigma(\lambda)\sqrt{2\pi r_o H}$$

where $\tau_o(\lambda)$ is the slant optical depth at the reference height r_o, $\tau_s(\lambda)$ is the slant optical depth at r, H is the scale height, (assumed constant over various height intervals in the atmosphere) and $\sigma(\lambda)$ is the absorption cross section.

Direct application of (2) to transmission curves for photon rates [see Smith et al. 1982] in the wavelength regions 550-615 Å and 661-717 Å gives a scale height of about 205 km. This implies a temperature T ~ 450 K, assuming H_2 is the dominant absorber and a number density at the τ_s = 1 level of 1.8 x 10^8 cm^{-3} in the 550-615 Å region. Since both the gravitational figure and the local gravity of Saturn vary significantly with latitude, reference altitudes and height scales can be very different at different latitudes. In order to avoid confusion and to facilitate intercomparison of the occultation results, we have, where possible, consistently used the equatorial latitude as a reference latitude and referred all altitudes to the 1 bar level above the equator. We have assumed this level to be at an absolute radius of 60263 km. The results of the measurements have been transformed so that they correspond to the reference latitude and level. Thus the τ_s = 1 level referred to is 2400 km above the 1 bar level at the equator.

We have modeled the solar occultation experiment by using a solar reference spectrum and assuming a photometrically uniform sun [Smith et al., 1982]. If the photometry of the sun at our wavelengths is spatially random, as it probably is [Reeves and Parkinson, 1970], this assumption should not lead to serious errors because the atmosphere and the instrument are averaging slices of the sun at a particular altitude. We estimate that if there are no extremely strong nonrandom photometric irregularities, smaller than 1/4 the scale height of the atmosphere (~50 km) then no serious errors should be made. The total time of the occultation was about 10 min so that variations in signal due to solar activity should be relatively minor. Using the above temperatures as starting points we have modeled various isothermal H_2 atmospheres from 3300 km down to 996 km. The modeling process allows the solar spectrum, with a spectral resolution of 1 Å, and the sun of proper size (150 km), to be attenuated by the model atmosphere as it descends through the atmosphere at 19.2 km/s. To this attenuated flux is applied instrument calibration, instrumental scattering and nonlinear instrumental current limiting and saturation effects [see Smith et al., 1982; and Shemansky et al., 1979]. The results of this process are shown in Figure 5. The data are shown as solid lines and the various models are indicated in the figure. The temperature appears to be between 400 and 450 K down to 1800 km in the 569-615 Å region, with 450 K giving overall the best fit. In each of the models we have varied the density so that the τ_s (569-615 Å) = 1 level is at the same altitude of 2200 km, thus the column amounts above and below this level are different for the different temperature models. This level refers to the 29.5° latitude region of the solar occultation. We have adjusted the models so that the transmission curves at 569-615 Å fit the data best, thus establishing the exact altitude reference between each model and the data. An earlier analysis [Festou and Atreya, 1982], using only

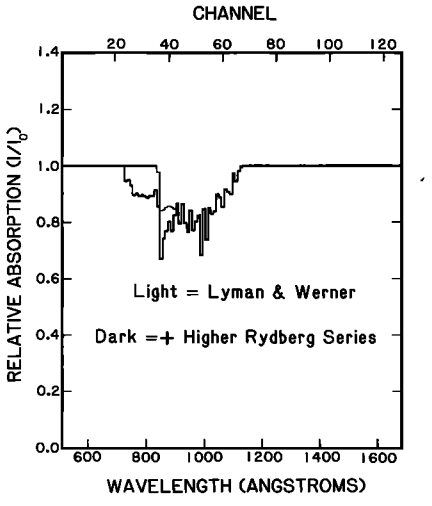

Fig. 6. Calculations of the relative absorption (I/I_o) for the H_2 bands where the column amount was 1.0×10^{19} cm^{-2} and the temperature was 375 K. The light curve represents absorption due only to the Lyman and Werner bands. The dark curve represents absorption of the Lyman and Werner bands plus the higher Rydberg series. Differences are significant below 900 Å.

the δ-Sco data, derived a temperature of 800^{+150}_{-120} K down to the 1540 km level above 1-bar. We believe this result is erroneous for reasons discussed below. As a comparison we have modeled an 800 K atmosphere (Figure 5) to show that a temperature of this magnitude is obviously not compatible with the solar data. We show later that an 800 K atmosphere is also incompatible with the δ-Sco occultation data.

Spectral Region from 912 Å to 1150 Å

Both the stellar and solar sources have significant flux in this region of the spectrum. The most likely absorbers are H_2 and CH_4. In Figure 4 we show I/I_o data versus time for the 939-1041 Å region of the stellar occultation. There is a slow attenuation of the signal down to where $I/I_o \simeq .37$ at about 1020 km. Below this level the signal decreases at a much greater rate implying the presence of a different absorber with smaller scale height and/or a rapid change in temperature at and below this point. This also appears to be the case in the solar data as shown in Figure 3.

Analysis of the upper portion of these data can proceed if we have realistic values for the absorption due to the H_2 bands in this spectral region. We have calculated the absorption of the H_2 bands by using the method described by Festou et al. [1981]. In our calculation, however, we have made the important addition of the four Rydberg band systems described by Shemansky and Ajello [1983]. Figure 6 shows the effect of these additional bands on the transmission for a 1.0×10^{19} cm^{-2} column of H_2 molecules at a temperature of 375 K. These four bands shift the peak of the absorption from 1000 Å to below 900 Å and add additional absorption from about 950 Å shortward to 725 Å. We implemented the H_2 band absorption into the modeling process by calculating a matrix of average absorption values for temperature, column amount, and wavelength. The temperatures ranged from 1000 K to 100 K in steps of 200 K down to 200 K. The column amounts ranged from 1.0×10^{18} cm^{-2} to 1.0×10^{21} cm^{-2}. We first calculated the absorption at a resolution of 0.1 Å over the wavelength range of 725 Å to 1150 Å then reduced the resolution (or averaged) to 9.26 Å to match the instrumental channel width. We then interpolated within this matrix to find the absorption of the model atmosphere. This procedure for non-isothermal atmospheres possesses some uncertainty related to the temperature, which is chosen in the calculation to be the temperature at the densest point along the column. The alternative of calculating the contribution of small segments along the column including the effect of a changing line shape is prohibitive because of the calculation time involved.

The stellar occultation modeling process is similar to the solar's except that there are no nonlinear limiting effects to consider in the photon-counting mode in which the data were acquired. The results of modeling the 400 K and 450 K H_2 atmosphere for the solar occultation are compared with the data in Figure 5 for the wavelengths 958-1004 Å. In Figure 7 we show the 400 K, 450 K, and 800 K atmospheres compared with the δ-Sco stellar occultation for the wavelengths 939-1041 Å. These models are the same as the models shown in Figure 5 where we have transformed the models from the solar occultation latitude (29.5°) to the stellar occultation latitude (3.8°). Thus at the same gravitational potential level the pressures are the same for the same temperature model. We note that the altitude scales of Figures 5 and 7 are for different latitudes and cannot be compared directly. The H_2 band data from the δ-Sco occultation is clearly consistent with the H_2 continuum and H_2 band data from the solar occultation and implies a temperature between 400 K and 450 K down to about 1100 km above the 1 bar level. It would appear that the 400 K model is a slightly better fit to the stellar data than the 450 K model. The 800 K model obviously does not fit the data well even at 1540 km. Below 1100 km we must consider the hydrocarbon absorbers.

The Hydrocarbon Region

Compared to the analysis of the data in the thermosphere, the analysis near the mesopause region, where the hydrocarbons are beginning to absorb and radiate, is rather difficult. In the thermosphere basically two parameters are needed, the temperature and a column amount at one altitude level, because the atmosphere is nearly isothermal. Once a column amount is derived for a particular altitude the temperature is varied until a fit to the data is obtained. In the region of the mesopause the temperature is no longer iosthermal [Strobel and Smith, 1973] and the atmosphere changes from being diffusively separated to a uniformly mixed one.

The parameterization of this change from a mixed to a diffusively separated atmosphere was given by Colegrove et al. [1965] and can be

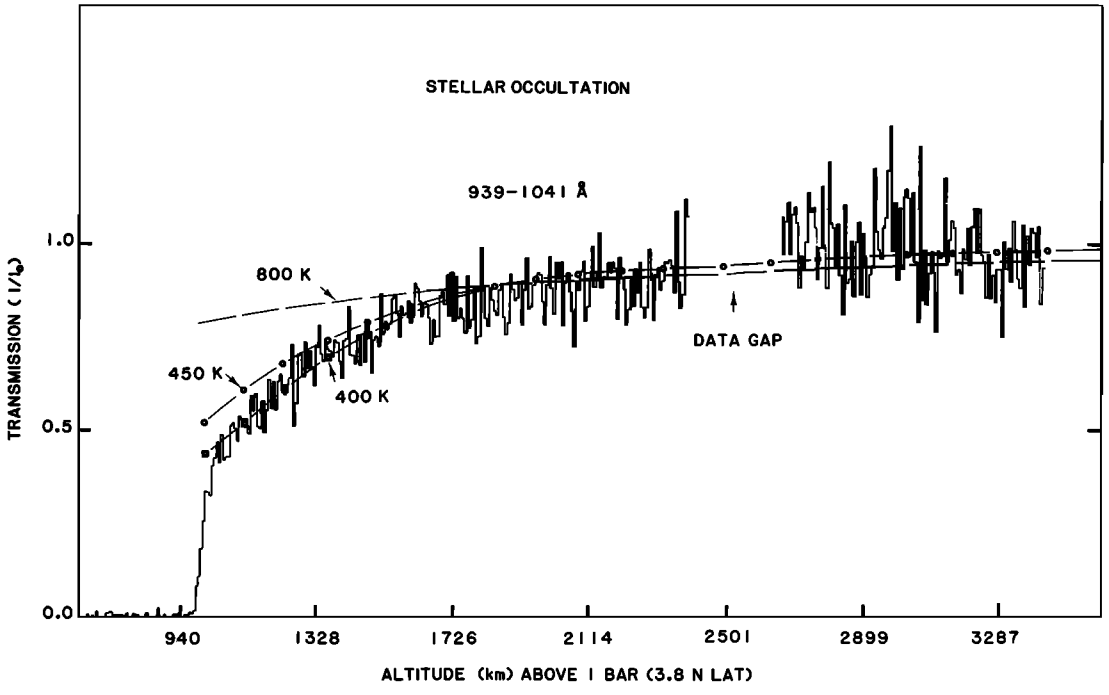

Fig. 7. Comparison of 400 K, 450 K, and 800 K models with the Voyager 2 stellar occultation data from the wavelength region 939–1041 Å. The data and models are given as transmission curves as a function of altitude above the 1-bar level at 3.8° N latitude. The data are a solid curve plotted as a histogram with each point containing the information from two spectra over an altitude extent of about 6.5 km. The isothermal models are 450 K (open circles), 400 K (squares), and 800 K (dashed line). These models are the same as shown in Figure 5 where they have been transformed to the 3.8° N latitude region (see text). Above 1900 km there is little difference in the 400 K and 450 K models.

written without thermal diffusion as

$$\phi_i = -D_i \left[\frac{dn_i}{dz} + \frac{n_i}{H_i} + \frac{1}{T}\frac{dT}{dz}\right] - K\left[\frac{dn_i}{dz} + \frac{n}{H_a} + \frac{1}{T}\frac{dT}{dz}\right] \qquad (3)$$

where ϕ_i is the flux and n_i the density respectively of the i^{th} constituent, D_i is the binary diffusion coefficient in H_2, H_i and H_a are the scale heights of the i^{th} constituent and the background atmosphere, respectively, and K is the eddy diffusion coefficient. In order to model a minor constituent, (3) must be solved using continuity equations if there are sources and sinks other than boundary conditions for n_i and ϕ_i.

Detailed photochemical studies [Strobel, 1978; Yung and Strobel, 1980; Ashihara 1983] where (3) has been solved assuming isothermal conditions with constant and variable K have shown that CH_4 should be the primary hydrocarbon in the upper atmosphere. We thus assume in the following that CH_4 is the primary hydrocarbon absorber at the levels above 960 km. In order to model this region, even in a simple manner, we need estimates of the temperature, the column amount or mixing ratio of CH_4 at some altitude level, and the eddy diffusion coefficient.

Sandel et al. [1982a] and Atreya [1982] have obtained estimates of the eddy diffusion coefficient by using the δ-Sco data in conjunction with other data. Sandel et al. [1982a] used the δ-Sco data and the UVS He 584 Å airglow data assuming an isothermal atmosphere and constant eddy profile and found $K = 8 \pm 4 \times 10^7$ cm² s⁻¹. Atreya [1982] found a similar result, based on photochemical model calculations [Festou and Atreya, 1982] and calculations of atomic hydrogen production by Waite [see Atreya, 1982]. The Festou and Atreya [1982] calculations must have included an estimate of the eddy diffusion coefficient in the first instance, but the matter is not discussed in the paper. Both calculations presumably have a dependence on an assumed CH_4 mixing ratio below the homopause.

A constituent that has a reasonably large difference in cross section at different wavelengths will also have an altitude shift at the same optical depth. We use this effect to obtain information about the height variation of the absorber in the region below 1200 km. Assuming isothermal conditions and using (2), we get a relation between cross section and the effective scale height as

$$H_{eff} = -(z_2 - z_1)/\ln(\sigma_1/\sigma_2), \qquad (4)$$

where $z_2 > z_1$. We call this the effective scale height because the actual scale height of the minor constituent in the transition region between the fully mixed and the diffusively separated region is between H_a and H_i even

without photochemical sources and sinks. Using the data from 1273-1347 Å and the data shown in Figure 4, we obtain an altitude shift of 19-26 km. The ratio of the cross sections of CH_4 in these two wavelength regions is about 3.7 [Hudson, 1971]. Using these values in (3) gives $H_{eff} \simeq 14.5$-19.9 km. Analyzing the transmission curves from each region separately we obtain $H_{eff} \simeq 12 \pm 2$ km.

Using (4) of Wallace and Hunten [1973] we derive a relation between H_{eff} and H_a in the atmosphere that can then give an estimate of the temperature near the CH_4 homopause. The relation is

$$H_a = H_{eff}\left[\frac{1 + se^h}{1 + e^h}\right] \qquad (5)$$

where $h = (z - z_o)/H_a$, $s = H_a/H_{CH_4}$, and z_o is the location of the methane homopause. Using the H_{eff} derived above, we obtain temperatures from 90 K to 180 K. Sandel et al. [1982a] derived a temperature of 125^{+40}_{-25} K and Festou and Atreya [1982] obtained 140^{+35}_{-25} K.

We emphasize at this point that the basic data obtained from the occultation experiments are transmission of the atmosphere at various wavelengths as a function of altitude or radial distance from Saturn's center. Thus if one constituent is the primary absorber and its cross section is known we can relate transmission to slant column amounts. If we are considering data in the region of transition from mixed to diffusively separated we cannot relate the slant column amounts to local density or vertical column amounts without resorting to a model since the densities are changing in an unknown manner with altitude. A full model basically requires three of the four parameters: temperature, mixing ratio deep in the atmosphere, eddy diffusion coefficient, and a slant column amount high in the atmosphere. The temperature and the eddy diffusion coefficient as shown above are very uncertain. The mixing ratio deep in the atmosphere is also quite uncertain, $1.85^{+1.2}_{-0.5} \times 10^{-3}$, according to Courtain et al. [1982]. The value given by Hanel et al. [1981] (8×10^{-4}) is an assumed value (see Table 1 in Hanel et al. [1981] and J. Pearl (private communication 1982)). Thus the only values that are reasonably fixed by any observation are the transmissions or slant column amounts over an altitude range of ~60 km derived from the UVS occultations. Because of the large variation in the parameters needed for a complete modeling process our approach was to try to fit the data in the region below 1200 km with three different models in order to refine the possibilities.

A Bates model [Bates, 1959] was used from the upper atmosphere down to 996 km where the base temperature is 90 K, 120 K, and 150 K, respectively for the three models tested. These temperatures reasonably bracket the values obtained above. At the upper levels we used 420 K and a $dT/dz_o(z_o = 996)$ of 2.0 K/km. The lapse rate is not well determined. However, if this quantity is too small, the H_2 densities in the lower regions become excessively large because the densities high in the atmosphere are already fixed by the H_2 continuum and band data. Below 996 km the atmosphere is assumed isothermal down to 960 km, where the modeling stops. In each model we fixed the level of τ_s(1273-1347 Å) = 1 for CH_4 at the altitude of ~983 km, as constrained by the UVS data. For each of the above temperature models (90 K, 120 K, 150 K) we solved (3) with constant eddy diffusion coefficients of 5.0×10^6 cm^2 s^{-1} and 1.0×10^8 cm^2 s^{-1} and compared the results with the data from 939-1041 Å and 1273-1347 Å. The difference between the models varied little with temperature, so we only show the result for one temperature, T = 120 K, in Figure 8. The solid curves represent the data, and the dashed curves are the results of the model. The model with $K = 1.0 \times 10^8$ cm^2 s^{-1} appears definitely inconsistent with the 939-1041 Å data anywhere in the altitude region below 1100 km, whereas the model with $K = 5.0 \times 10^6$ cm^2 s^{-1} appears quite satisfactory. The fit in the 1272-1347 Å region also favors the model with $K = 5.0 \times 10^6$. A model with $K = 2.5 \times 10^7$ cm^2 s^{-1} was also compared with the data and was found to have an unsatisfactory fit to the data. It appears that $K < 2.5 \times 10^7$ cm^2 s^{-1} with $K = 5.0 \times 10^6$ cm^2 s^{-1} being the prefered value. Further detailed modeling must be carried out in order to define the precise range of acceptable K and temperature.

Atomic Hydrogen

Adding various abundances of H to the 400 and 450 K hydrostatic H_2 models previously derived provides a reasonable fit to the 865-912 Å data down to about 1600 km as shown in Figure 9. Below 1600 km the H distribution in the diffusively separated model deviates from the observations, indicating larger amounts of H in the models than are actually present if the upper regions are used as a point of reference. The simplest way to correct for this effect and thus fit the data is by introducing a downward flow of H. Since the fit at 2300 km is satisfactory, we fixed the column amount of H at this level in the 450 K model and solved (3) with $K = 5.0 \times 10^6$ cm^2 s^{-1} with various amounts of downward H flux as a boundary condition. With a downward flux of 1.8×10^9 cm^{-2} s^{-1} we obtained the result shown in Figure 9. The model with this amount of flux fits somewhat better than the zero flux models in the region from 1600 km to about 1100 km. Below 1100 km the hydrocarbons will be significant contributors to the extinction of the radiation since the cross sections are larger than the H cross sections by about an order of magnitude. The downward flux indicated here that seems to be necessary to fit the observed H profile implies that in some higher altitude region we must have a source of atomic hydrogen. We discuss this in quantitative terms in the following section.

Discussion

The value for the temperature in Saturn's upper atmosphere derived in this paper is nearly a factor of 2 less than that arrived at by Festou and Atreya [1982]. The solar Voyager 2 occultation at Saturn has produced a very acceptable data set, unambiguous in its interpretation, especially in the H_2 continuum region at high altitudes, and we were able to directly derive a temperature from the data assuming a single constituent model. Further modeling of the solar

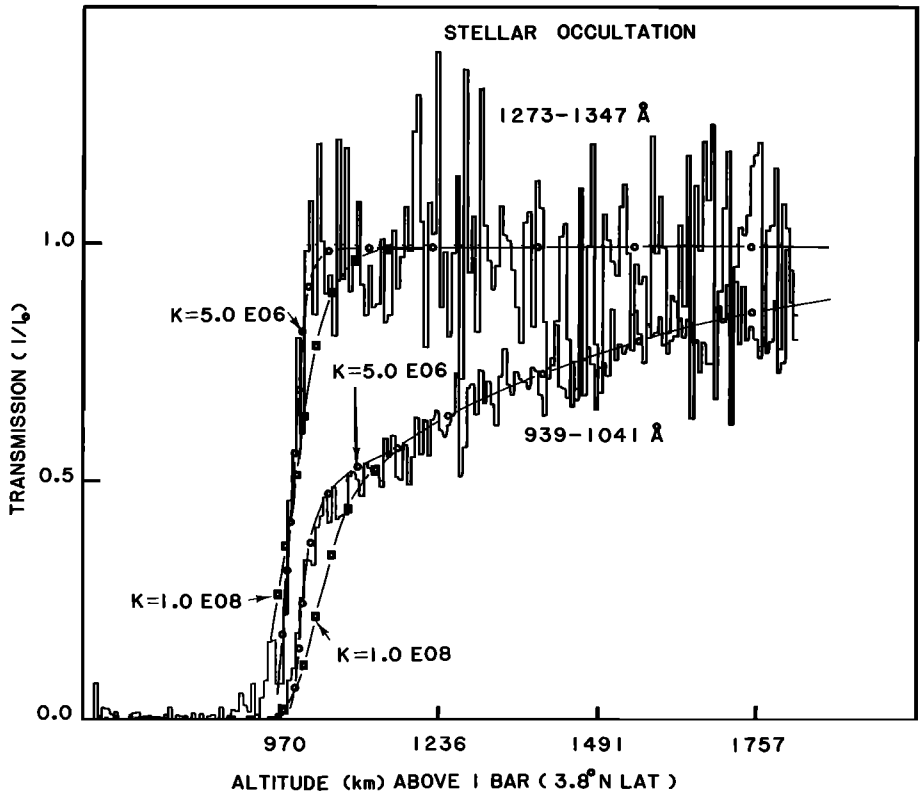

Fig. 8. Comparison of two models with different eddy diffusion coefficients with δ-Sco stellar occultation data. The data are shown as solid histograms with each point containing the information from two spectra or about 6.5 km. The models are Bates models where T_∞ = 420 K, $T_0(z_0$ = 996 km) = 120 K, below 996 km T = 120 K down to 960 km. A lapse rate of 2.0 K/km at 996 km was used. The only difference in the models was the eddy diffusion coefficient used. The column amounts of CH_4 at 983 km were the same in both models. The model with K = 5.0 x 10^6 cm^2 s^{-1} is shown as open circles and the model with K = 1.0 x 10^8 cm^2 s^{-1} is shown as squares. Above about 1200 km the two models give identical results.

and stellar occultations has confirmed this and an earlier estimate [Sandel et al. 1982b]. In the case of the stellar occultation data, information on the atmospheric structure can only be obtained by discrete absorption due to the H_2 bands. Because of the nature of the discrete absorption process [see Goody, 1964] it is very difficult to determine, from a limited altitude region, precisely the area of the curve of growth to which the data applies. As seen from Figure 7 one could obtain a reasonable fit to the data with an 800 K atmosphere down to about 1540 km by shifting the model curve in altitude relative to the data. However, if one considers the data over the total range in altitude (Sandel et al. [1982b] and Figure 7) it becomes obvious which temperature is correct. This is because the temperature difference is manifested through the total 'scale' of the atmosphere where the local scale height difference enhances the slant column amount variation exponentially with altitude.

Our modeling and analysis of the data seems to indicate that the eddy diffusion coefficient is lower than previous estimates [Sandel et al., 1982a; Atreya, 1982]. Our differences with Sandel et al. [1982a] could possibly be explained by the application of different temperatures and by the fact that totally different wavelength regions were used in the analyses. Our CH_4 number density mixing ratio, given in the abstract, of 6 x 10^{-5} has errors of ±4 x 10^{-5} associated with it due to the uncertainty of the temperature used at the lower boundary in our models. If we extrapolate this result into the lower atmosphere, we disagree with the Hanel et al. [1981] assumed value of 8 x 10^{-4} by a factor of at least 3. The CH_4 mixing ratio given by Courtain et al. [1982] is in reasonable agreement with our models for values of the temperature of the lower boundary (960-996 km) between 90 K and 120 K. This may indicate that the temperature near the mesopause is less than 120 K. However, more extensive photochemical modeling and analysis of the data in the longer wavelength regions must be carried out before more exact values can be determined for the temperature and the eddy diffusion coefficient.

The source of the atomic hydrogen flux that has been derived above as a means of accounting for the observed hydrogen altitude profile, probably arises mostly in the region near the exobase at ~2500 km. We base this statement on the observation of H_2 band emission from the sunlit equatorial region, which according to Shemansky and Ajello [1983] is dominated by a source just below the exobase. A relatively weaker source is expected to arise deeper in the atmosphere produced by photoelectron collisions.

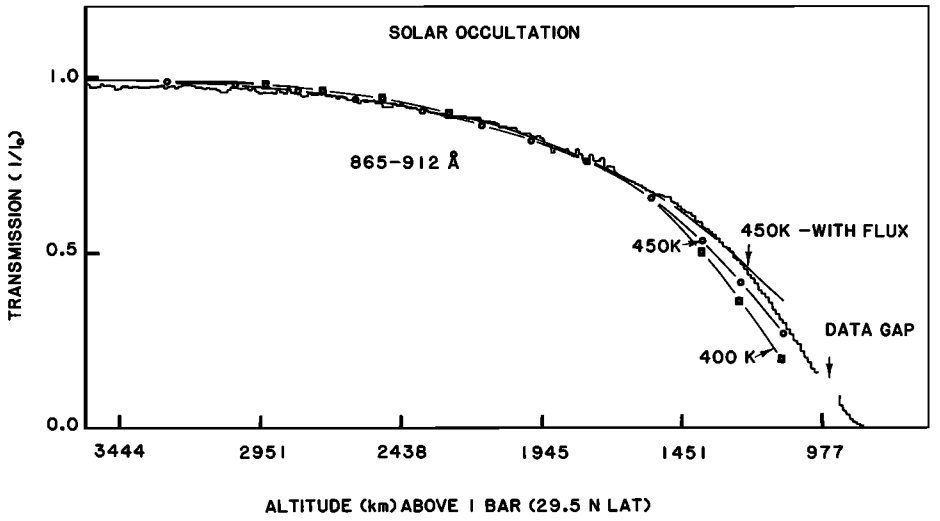

Fig. 9. We compare the solar data from 865-912 Å with 450 K (open circles) and 400 K (squares) isothermal models. These models represent the same H_2 atmospheres as shown in Figure 5, where atomic hydrogen has now been added. The curve shown as a dashed line marked 450 K with flux is a model with a downward flux of 1.8 x 10^9 cm^{-2} s^{-1} of H atoms. The column amount at 2300 km was held the same as the 450 K model without flux.

A more refined analysis (D.E. Shemansky and G.R. Smith (unpublished manuscript, 1983)) indicates that the equatorial H_2 band emission is actually slightly higher in the exobase region than the depth given by Shemansky and Ajello, and in addition shows that the mean energy of the exciting electrons is roughly 30 eV. The estimated column ionization rate and production of H atoms by neutral dissociation is ~9 x 10^8 cm^{-2} s^{-1} and ~1.1 x 10^9 cm^{-2} s^{-1} respectively, on this basis (D.E. Shemansky and G.R. Smith (unpublished manuscript, 1983)). In addition to the source of neutral atoms produced directly by electron impact, we have a source caused by subsequent dissociative recombination reactions. The primary electron reaction produces H_2^+, which rapidly reacts with H_2,

$$H_2^+ + H_2 \rightarrow H_3^+ + H$$

followed by,

$$H_3^+ + e \rightarrow 3H$$

or $$\rightarrow H_2 + H$$

The production of atomic hydrogen by this indirect process in steady state is thus between 1 and 2 times the electron ionization rate. Thus the total column production of H, and hence downward flux, would be about 2 to 3 x 10^9 cm^{-2} s^{-1}. This then would give a globally averaged value of 5.0 to 7.5 x 10^8 cm^{-2} s^{-1}. Adding this value to that produced by photoionization [Strobel, 1978] gives 1-2 x 10^9 cm^{-2} s^{-1}. The agreement with the value derived from the data is quite good.

Since we have measured the temperature in the thermosphere and have an estimate near the mesopause, it is of interest to use the results of Strobel and Smith [1973] to estimate the energy deposition in the thermosphere required to give the observed temperature rise. The observed temperature rise is about 300 K, while the temperature rise due to photoionization is about 10 K [Strobel and Smith, 1973], so we neglect the effects due to photoionization and will consider only heating by electrons. With the thermal conductivity given as AT^s where A = 252 ergs (cm s K)$^{-1}$ and s = .751 [Hanley et al., 1970], the heating term can be written

$$Q_e = \frac{A}{(s+1)(z_e - z_o)}(T_\infty^{s+1} - T_m^{s+1}) \qquad (6)$$

where $z_e - z_o$ is the separation in altitude between the heating location and the area of cooling, idealized to be single locations in the atmosphere. For photoionization $(z_e - z_o)$ was found to be about 5 H_a, [Strobel and Smith, 1973], where H_a referred to the thermospheric scale height. However, if we assume most of the energy enters at 2500 km, as the emission data suggest, then the separation distance between source and sink is $z_e - z_o$ = 2500 - 1000 = 1500 km, or 7 H_a, these values in (6) give

$$Q_e = 0.033 \pm .003 \text{ ergs } cm^{-2} s^{-1} \qquad (7)$$

This requirement for energy deposition based on the temperature differential across the thermosphere can be compared with the deposition rate implied by the observation of H_2 band emission from the exobase region. A complicating factor in making such an estimate lies in the uncertainty in the exact nature of the deposition process (D.E. Shemansky and G.R. Smith (unpublished manuscript, 1983)). A common method of calculating the estimated total electron energy deposition in auroral deposition processes is through the known ionization efficiency of 2.8 x 10^{-2} electron-ion pairs per eV of electron energy loss [Valentine and Curran, 1958]. An estimate on this basis implies the assumption that the electrons in the excitation process lose all of their energy in the locally observed volume. In this particular case a calculation on the basis

of total electron energy deposition apparently is not appropriate, but only represents the minimum energy deposition rate (D.E. Shemansky and G.R. Smith (unpublished manuscript, 1983)), 0.046 ergs cm^{-2} s^{-1} in the equatorial region. However, the total energy flux in the exciting electrons is estimated to be an order of magnitude larger, ~0.26 ergs cm^{-2} s^{-1} (D.E. Shemansky and G.R. Smith (unpublished manuscript, 1983)). The excitation process therefore cannot be strictly described as an auroral type deposition process, and the actual energy deposition rate in the equatorial region must be somewhere between the extremes 0.26 and 0.046 ergs cm^{-2} s^{-1}. The fraction of the electron energy ultimately deposited as local heating therefore ranges somewhere between 92% and 53% (D.E. Shemansky and G.R. Smith (unpublished manuscript, 1983)), and it is entirely reasonable that the observed source at 2500 km could account for the thermospheric temperature. The deposition of heat energy in the 2500-2300 km region through the flux of energetic atomic hydrogen implies that the atmosphere should show a thermal gradient from at least the 2300 km level downward. In this case the model calculations have assumed an isothermal thermosphere down to ~1600 km. Although we have not actually included a gradient in the upper region, it appears that a moderate gradient could be tolerated as required by a .032 ergs cm^{-2} s^{-1} deposition in the 2500- to 2300- km range. A more refined calculation of heat balance and thermal structure should be carried out to examine this question further but is beyond the scope of this paper.

Summary

Analysis of the occultations of the sun and the star δ-scorpii has enabled us to make estimates of the temperature and composition of the upper atmosphere of Saturn. Even though the solar and stellar occultations were observed at different latitudes we feel that a representative temperature for both observations is 420 ± 30 K for the upper atmosphere above about 1600 km. Below this the temperature decreases down to 120 ± 30 K in the region of 990 km. Column amounts of H and H_2 were directly measured down to about 1100 km. In order to obtain the best fit to the H continuum data a downward flux of ~1.8 x 10^9 cm^{-2} is needed.

By assuming that the absorber in the 939-1041 Å region at lower altitudes is CH_4 and using the 1273-1347 Å region we have inferred CH_4 densities in the lower regions below 1100 km Using the information derived from the H_2 analysis and modeling, we suggest that the eddy diffusion coefficient near the homopause is about 5.0 x 10^6 cm^2 s^{-1}. In Figure 10 we give the preferred model of Saturn's atmosphere above 960 km for the three constituents H, H_2, and CH_4 along with the temperature. We used a Bates model as explained above with T_{inf} = 420 K, T_0 = 120 K at 996 km and isothermal below to 960 km. The lapse rate was 2.0 K/km at 996 km and the eddy diffusion coefficient was constant with the value 5.0 x 10^6 cm^2 s^{-1}. For atomic hydrogen a downward flux of 1.8 x 10^9 cm^{-2} was used. The height scale is referred to the 60263 km level above the equator, assumed to be the 1-bar level.

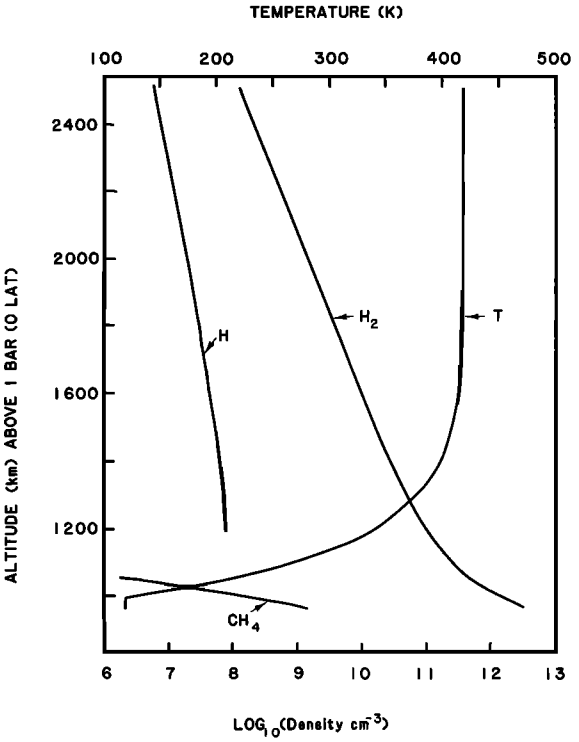

Fig. 10. The preferred model of Saturn's upper atmosphere is shown transformed to the equatorial region and referred to the 1-bar level at the equator assumed to be at 60263 km above Saturn's center. The upper atmospheric temperature is 420 K decreaseing to 120 K at 996 km, below this it is isothermal to 960 km. The eddy diffusion coefficient used was 5.0 x 10^6 cm^2 s^{-1}. The profile for H was derived with a downward flux of 1.8 x 10^9 cm^{-2} s^{-1} of H atoms.

The temperature uncertainty of ± 30 K for the upper atmosphere and the data do not exclude the possibility of a temperature gradient above 1600 km.

Acknowledgements. The Editor thanks G.H. Mount and J.H. Waite for their assistance in evaluating this paper. The authors acknowledge the assistance of T.P. McBreen and W.T. Forrester in the processing of the Saturn occultation data. This work was supported by the Jet Propulsion Laboratory under NASA contract NAS7-100. Additional support was provided by NASA's Office of Space Sciences under contracts NAGW-161 and NAGW-62.

References

Ashihara, O., Methane photochemistry in the outer planets, The Inst. of Space and Astronaut. Sci., Tokyo, Rep. N. 602, 1983.

Atreya, A. K., Eddy mixing coefficient on Saturn, Planet. Space Sci., 30, 849-854, 1982.

Bates, D. R., Some problems concerning the terrestrial atmosphere above about 100 km level, Proc. R. Soc. London Ser. A, 253, 451, 1959.

Broadfoot, A. L., et al., Ultraviolet spectrometer experiment for the Voyager mission, Space Sci. Rev., 21, 183, 1977.

Broadfoot, A. L., et al., Extreme ultraviolet

observations from Voyager 1 encounter with Saturn, Science, 212, 206, 1981.
Chamberlain, J. W., Planetary coronae and atmospheric evaporation, Planet. Space Sci., 11, 901, 1963.
Courtin, R., J. P. Baluteau, D. Gautier, A. Marten, and W. Maguire, The minor constituents of Saturn's atmosphere from the Voyager 1 IRIS experiment, paper presented at the Saturn meeting, University of Arizona, Tucson, Arizona, May 12, 1982.
Colegrove, F. D., W. B. Hanson, and F. S. Johnson, Eddy diffusion and oxygen transport in the lower thermosphere, J. Geophys. Res., 70, 4931, 1965.
Festou, M. C. and S. K. Atreya, Voyager ultraviolet stellar occultation measurements of the composition and thermal profiles of the Saturnian upper atmosphere, Geophys. Res. Lett., 9, 1147-1150, 1982.
Festou, M. C., S. K. Atreya, T. M. Donahue, B. R. Sandel, D. E. Shemansky, and A. L. Broadfoot, Composition and thermal profiles of the Jovian upper atmosphere determined by the Voyager ultraviolet stellar occultation experiment, J. Geophys. Res., 86, 5715, 1981.
Gillet, F. C. and W. J. Forrest, The 7.5 to 13.5 micron spectrum of Saturn, Astrophys. J., 187, L37-L39, 1974.
Goody, R. M., Atmospheric Radiation, Oxford Monographs on Meteorology, edited by P.A. Sheppard, Oxford at the Clarendon Press, London, 1964.
Hanel, R., B. Conrath, F. M. Flosar, V. Kundi, W. Maguire, J. Pearl, J. Perraglia, R. Samuelson, L. Herath, M. Allison, D. Crukshank, D. Gautier, P. Gierasch, L. Horn, R. Koppany, and C. Ponnamperuma, Infrared observations of the Saturian system from Voyager 1, Science, 212, 192, 1981.
Hanley, H. J. M., R. D. McCarthy, and H. Inteman, The viscosity and thermal conductivity of dilute gaseous hydrogen from 15 to 5000 K, J. Res. Nat. Bur. Stand., 74A, 331, 1970.
Holberg, J. B., W. T. Forrester, and J. J. Lissauer, Identification of resonance features within the rings of Saturn, Nature, 297, 115-120, 1982a.
Holberg, J. B., W. T. Forrester, D. E. Shemansky and D. C. Barry, Voyager absolute far-ultraviolet spectrophotometry of hot stars, Astrophys. J., 257, 656, 1982b.
Hudson, R. D., Critical review of ultraviolet photoabsorption cross sections for molecules of astrophysical and aeronomic interest, Rev. Geophys. Space. Phys., 9, 305, 1971.
Kliore, A. J., I. R. Patel, G. F. Lindal, D. N. Sweetnam, H. B. Hotz, J. H. W. Waite, and T. R. McDonough, Structure of the ionosphere and atmosphere of Saturn from Pioneer 11 Saturn radio occultation, J. Geophys. Res., 85, 5827, 1980.
Kuiper, G. P., Planetary atmospheres and their origins, p. 306 in The Atmospheres of the Earth and Planets, revised edition, University of Chicago Press, Chicago, Ill., 1952.
Moos, H. W., and J. T. Clarke, Detection of acetylene in the Saturion atmosphere using the IUE satellite, Astrophys. J. Lett., 229, L107-L108, 1979.
Munch, G., and H. Spinrad, On the spectrum of Saturn, Mem. Soc. R. Sci. Liege, Vol. Hors Ser, 541, 1963.
Orton, G. S. and A. P. Ingersoll, Saturn's atmosphere temperature structure and heat budget, J. Geophys. Res., 85, 5871, 1980.
Reeves, E. M., and W. H. Parkinson, An atlas of extreme-ultraviolet spectroheliograms from OSO-IV, Astrophys. J. Suppl., 21, 1-31, 1970.
Sandel, B. R., J. C. McConnell, and D.F. Strobel, Eddy diffusion at Saturn's homopause, Geophys. Res. Lett., 9, 1077, 1982a.
Sandel, B. R., D. E. Shemansky, A. L. Broadfoot, J. B. Holberg, G. R. Smith, J. C. McConnell, D. F. Strobel, S. K. Atreya, T. M. Donahue, H. W. Moos, D. M. Hunten, R. B. Pomphrey, S. Linick, Extreme ultraviolet observations from the Voyager 2 encounter with Saturn, Science, 215, 548, 1982b.
Shemansky, D. E., and J. M. Ajello, The Saturn spectrum in the EUV - electron excited hydrogen, J. Geophys. Res., 88, 459, 1983.
Shemansky, D. E., B. R. Sandel, and A. L. Broadfoot, Voyager observations of the interstellar medium in the 500 to 1700 Å spectral region, J. Geophys. Res., 84, 139, 1979.
Smith, G. R., D. F. Strobel, A. L. Broadfoot, B. R. Sandel, D. E. Shemansky, and J.B. Holberg, Titan's upper atmosphere: Composition and temperature from the EUV solar occultation results, J. Geophys. Res., 87, 1351, 1982.
Strobel, D. F., Aeronomy of Saturn and Titan, in The Saturn System, edited by D. M. Hunten and D. Morrison, NASA CP-2068, 1978.
Strobel, D. F., and G. R. Smith, On the temperature of the Jovian thermosphere, J. Atmos. Sci., 30, 718, 1973.
Tokunaga, A., The thermal structure of Saturn: Inferences from ground-based and airborne infrared observations, in The Saturn System, edited by D. M. Hunten and D. Morrison, NASA CP-2068, 1978.
Valentine, J. M. and S. C. Curran, Average energy expenditure per ion pair in gases and gas mixtures, Rep. Prog. Phys., 21, 1, 1958.
Wallace, L. and D. M. Hunten, The Lyman-Alpha albedo of Jupiter, Astrophys. J., 182, 1013, 1973.
Wildt, R., Absorptionsspectren und atmospharen der grossen planeten, Veroff. Univ. Sternwarte Gottingen, 22, 171, 1932.
Yung, Y. L., and D. F. Strobel, Hydrogen photochemistry and Lyman-alpha albedo of Jupiter, Astrophys. J., 239, 395, 1980.

Gerald R. Smith, D. E. Shemansky, J. B. Holberg, A. L. Broadfoot, and B. R. Sandel, Center for Space Sciences, University of Southern California, Tucson Laboratories, 3625 E. Ajo Way, Tucson, AZ 85713.

John C. McConnell, Department of Physics, York University, Downsview, Ontario, Canada, M3J 1P3.

(Received October 4, 1982;
revised May 26, 1983;
accepted May 26, 1983.)